Final Copy

AIAA

AIAA-99-1267
MICRODYNAMIC BEHAVIOR OF A JOINT DOMINATED STRUCTURE ON-ORBIT

M. B. Levine
California Institute of Technology
Jet Propulsion Lab
Pasadena CA

40th AIAA/ASCE/AHS/ASC Structures, Structural Dynamics, and Materials Conference
AIAA/ASME/AHS Adaptive Structures Forum
AIAA Forum on Non-Deterministic Approaches
Conference and Exhibit
12-15 April, 1999
St. Louis, Missouri

AIAA-99-1267

MICRODYNAMIC BEHAVIOR OF A JOINT DOMINATED STRUCTURE ON-ORBIT

Marie B. Levine
Interferometry Technology Program, Microdynamics
Jet Propulsion Laboratory, California Institute of Technology
4800 Oak Grove Drive, M.S. 157-316
Pasadena, CA 91109, USA

ABSTRACT

The Interferometry Program EXperiments (IPEX) I and II are the first free-flying space experiments specifically designed to characterize the sub-micron microdynamic behavior of large flexible optical structures subjected to on-orbit thermal-mechanical disturbances. These technology demonstration flight experiments are precursors to the 10-meter baseline Space Interferometry Mission (SIM) scheduled to launch in 2005, and will address the mission's nanometer-level structural stability requirements. The main objective of the flight experiments is to ascertain the existence of dynamic instabilities within mechanisms, joints and materials due to sudden internal strain energy redistribution such as thermal variations (a.k.a. thermal snap). This information is needed to characterize potentially uncontrollable vibrational disturbances, and to validate structural designs and modeling approaches for joint-dominated extruding structures. The data obtained from IPEX-II, performed aboard the ASTRO-SPAS during the Space Shuttle STS-85 mission in August 1997, assesses the characteristics of these dynamic instabilities on an actual joint-dominated flight structure. It is demonstrated that the flexible boom exhibited transient snaps as high as several mg peak-to-peak, but that the overall dynamic stability meets the SIM requirement of less than 10nm RMS above 100Hz.

1. INTRODUCTION

The objective of NASA's Origin Program is to address the fundamental questions of our place in the universe, such as how galaxies, suns and planetary systems form. Origins will use new technologies to investigate these questions with a suite of low-cost observatories in space and on the ground. These space missions are now in the planning and definition stages, and will be launched in the beginning of the new millennium.

The missions include the Space Interferometry Mission (SIM) , the Next Generation Space Telescope (NGST), and the Terrestrial Planet Finder (TPF), (Fig.1)

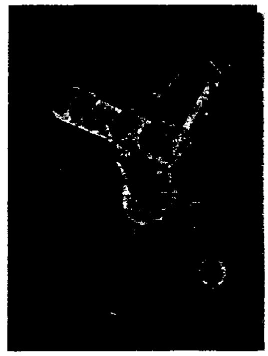

Figure 1. SIM "Classic" Design

One of the technologies that must be accomplished to meet the Origins science requirements is *nanometer* (10^{-9}m) level stabilization up to 1 kHz of the optical pathlength on light weight 10-meter to 100-meter class flexible structures. This stability requirement must be achieved while the observatory is experiencing spacecraft induced vibrations and transient thermal distortions. Most of the disturbances will be attenuated through vibration isolation at the mechanical disturbance source (e.g., reaction wheels) and through high-bandwidth optical pathlength control of the delay

Figure 2. IPEX-II boom on-orbit

lines and fast-steering mirrors. However, above the 300Hz bandwidth of the optical controller the open-loop mechanical jitter disturbances throughout the instrument must be below 10 nm RMS up to 1KHz. Of particular concern are the quasi-random pulse-like disturbances with high spectral content that are likely to occur when the spacecraft is subjected to instantaneous internal strain energy redistribution. Examples of phenomena leading to sharp strain energy variations include sudden temperature changes from sun eclipses or quasi-static mechanical load redistribution as the instrument moves large masses and applies large torques. Also, the successful implementation of vibration attenuation strategies require an *a-priori* knowledge of the vibration source characteristics, of the propagation of these disturbances throughout the structure, and of the dynamic properties of the structure in its zero-g operating conditions. These disturbance models, together with structural models, are required for integrated opto-thermo-mechanical disturbance prediction, instrument design, and science requirement verification.

However, little is actually known about the broadband high frequency (1 kHz) microdynamic behavior of large structures on orbit. Data from the Hubble Space Telescope demonstrated the existence of thermally induced snapping [2]. Some microgravity surveys were performed on orbiting space platforms, such as EURECA [3]. But, the objective of those measurements was to characterize the low-frequency behavior below 5HZ for verification of the microgravity science requirements, and did not address high frequency characterization of the dynamic behavior of the structures.

The *Interferometry Program Experiments*, IPEX-I and IPEX-II, took advantage of two ASTRO-SPAS (***S***huttle ***PA***llet ***S***atellite) flights, scheduled off STS-80 (November 1996) and STS-85 (August 1997) to gain more knowledge on the broadband mechanical and thermal behavior of actual space structures on orbit. IPEX-I characterized the vibrational environment of the A/S platform itself to determine whether it would meet the broadband nanometer stability requirements of a potential SIM technology demonstration flight. Details of ASTRO-SPAS (A/S), and results of the IPEX-I flight experiment are presented in [4].

2. IPEX-II EXPERIMENT DESIGN AND OBJECTIVES

The data obtained from IPEX-I was used to estimate the background disturbances for the follow-on flight experiment, IPEX-II, flown on STS-85 in August 1997. In IPEX-II, a 9-bay AEC-ABLE Deployable

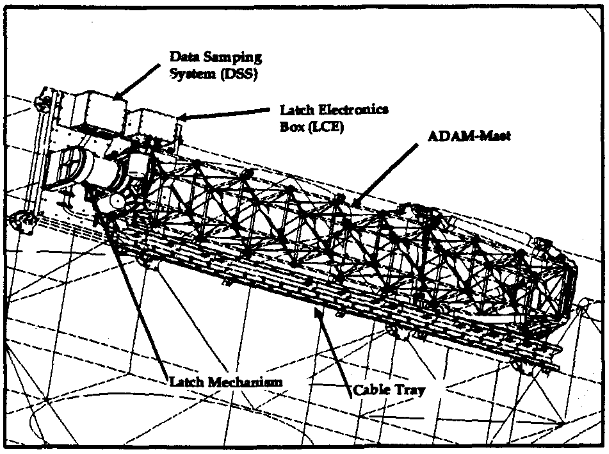

Figure 3. IPEX-II Boom Flight Configuration

Articulated Mast boom (ADAM), constructed from graphite composite and steel fittings, was cantilevered of the side of the A/S. The boom was instrumented with accelerometers, load cells, thermistors and shakers for complete on-orbit dynamic and thermal characterization of a potential Origins structural element. The boom was launched pre-deployed to avoid mechanical contamination from latch and deployment mechanisms (Fig.3). The objective of the IPEX-II experiment is to quantify the microdynamic stability of a potential structural element of an Origins structure. As in the case of IPEX-I, the prime concern is the existence of thermally induced snapping. Since the joints of the IPEX-II boom are heavily pre-loaded, the common belief prior to the flight was that snaps should not occur. Secondary objectives are the determination of the dynamic properties of the boom on-orbit and the propagation attenuation of known mechanical disturbances.

To meet these objectives, the instrumentation included 24 micro-g Sundstrand QA200accelerometers, 8 load cells, 42 temperature sensors, and 2 proof-mass shakers. A set of 6 accelerometers and 6 load cells were collocated inside the boom-to-spacecraft interface struts to characterize the 6 interface degrees-of-freedom. Sixteen accelerometers were installed along the boom, including 2 that were collocated with the 2 shakers and load cells at the tip of the boom. The shakers performed on-orbit modal tests to characterize the linearity and modal properties of the boom. The remaining 2 accelerometers were installed on the A/S to detect the source of the vibrations measured on the boom. The 48 temperature sensors were installed on the IPEX-II boom, of which 24 were inside the accelerometer casing for calibration purposes, 22 were collocated with the accelerometers to monitor the ambient temperature in the event of a thermal snap, and 2 were on either side of a boom strut to investigate thermal gradients across a structural member. Close to

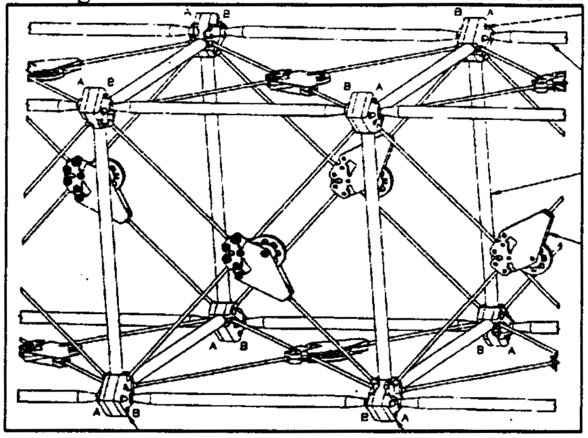

Figure 4. IPEX-II bay detail.

50 hours of on-orbit data was recorded at a 1 kHz sampling rate with 16-bit accuracy. Currently, the noise floor is estimated at 20μg RMS up to 500Hz, with 1μg RMS below 10Hz.The on-orbit tests are being followed by a suite of ground experiments and analyses performed at JPL, MIT and the University of Colorado at Boulder.

3. IPEX-II MECHANICAL DESCRIPTION

IPEX-II is an AEC-ABLE 9-bay ADAM boom that measures 2.3mx0.3mx0.3m. It is assembled of CFRP graphite battens and longerons, 440C steel ball fittings at the end of the struts, and 302/304 CRES steel cable diagonals with ball end-fittings to provide pre-load to the joints (Fig. 4). The ball joints rest in spherical socket with a nominal pre-load of 275 lbs. ± 25 lbs applied through steel cable cross brasses. The boom is launched pre-deployed, and the deployment clasp mechanisms within the cable pulley assemblies are restrained against motion with 2 fasteners.

The boom is cantilevered to the side of the A/S with 6 interface support struts providing a kinematic mount. Five of the support struts are made of graphite epoxy, and are less than 32" long. The sixth strut is made of titanium and is 4" long. The support struts are attached to the boom through an invar end plate to minimize the CTE (coefficient of thermal expansion) mismatch between the struts and the boom. Inside each of the support struts are 6 sets of collocated accelerometers and load cells to provide the full 6-dof representation of the A/S disturbance inputs into the boom. The free-end of the boom is restrained during launch and landing with a stow pin mechanisms, which is then opened during flight. The torsional rigidity of the boom is also maintained with an aluminum free-end plate through which the stow-pin passes, and to which 2 orthogonal shakers are attached to perform the on-orbit modal tests. Thermal MLI tape is applied locally to the boom joint fittings and to the pulley plates to minimize temperature gradients and material CTE mismatch. The sensor cables have service loops that minimize their stiffness coupling to the boom, and are fed down to a cable tray located just under the boom. The sensor signal conditioners are located inside the cable tray.

The total mass of the boom assembly is 38.9 Kg, which includes 13.3Kg for the boom, 9.4Kg for the fixed end plate, 2.2Kg for the free end plate, 9.9Kg for the support struts, 2.6Kg for the sensors and 1.5Kg for the 2 proof-mass actuators (PMA). The total mass of the Crista-Spas including all payloads exceeds 2000kg.

4. IPEX-II FLIGHT DATA RESULTS

4.1. Experiment Configuration

The 50 hours of on-orbit data was recorded in 5minute blocks at 20-minute to 9-minute intervals required for data download to the tape recorders. During the first 45 hours, the data recorded the response of the boom during A/S normal operation modes, including gyros, thrusters, and other payloads. This period also included over 25 day/night and night/day transitions. Furthermore, two experiments recorded at the slower sampling rate of 909Hz to identify any aliased response. The last 5 hours of the A/S flight were specifically dedicated to IPEX, and all other payloads were turned off. The most important experiment is a 5-minute segment when even the A/S gyros and thrusters were shut down, and the boom went through a sudden night to day transition. The only active mechanism on board was the tape recorder. This is the minimum disturbance state of the A/S, and is the period most likely to be quiet enough to measure thermally induced microdynamics in the boom. In addition, a total of 14 multi-shaker modal tests were performed to assess the on-orbit structural dynamic properties of the boom. Of special interest is the

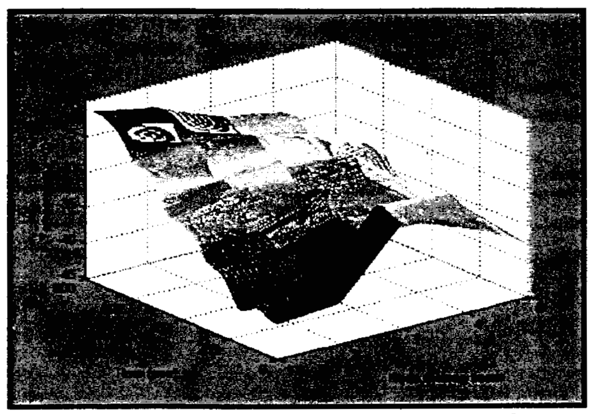

Figure 5. Temperature profile along one side of the boom during night/day transition.

change in damping. Two experiments were also dedicated to evaluating the boom response to specific A/S mechanical disturbances: gyro response without thrusters, and dedicated thruster pulsing sequence and direction with or without the gyros in the background. These tests will estimate the amount of disturbance propagation attenuation, a critical issue when predicting the response of the large precision structures to on-board disturbances.

More than 10 gigabytes of data has been collected during the flight experiment. At this time the data has not been completely analyzed, and the post-flight instrument calibration and verification have not yet been performed. The following is a synthesis of quiet time data that has been analyzed to date using pre-flight calibration information. A future report will update this data as necessary.

4.2. Thermal stability and microdynamics

At the beginning of the quiet period, during which all thrusters, gyros and payloads were turned off, the boom had been in complete shade for 1.5 hours, and the gyros had been shut down for 4.5 minutes. Except for the tape recorders, no mechanical or thermal disturbances were affecting the boom. Figure 5 shows the temperature response of sensors located on one side of the boom during that experiment. The boom was originally at –40°C, and increased to -20 °C at the end of this data sequence. By the time the next experiment starts recording, 10 minutes later, all sensors read a temperature of about 0°C.

Using the current orbital information for the A/S, a night to day transition was predicted to occur 30 seconds into the data. However, the temperature only starts rising at 60 seconds. It is not clear whether the delay in the temperature rise is due to a 30-second error in the transition estimate, a transient effect of the thermal mass, or a self-shadowing effect of the boom onto the sensor. Hence, for analysis purposes the data will be broken up into three parts, period 0sec to 30sec is the "night" data, 30sec to 70sec is the "transition" data, 70sec to 250 sec is the "day" data. Thrusters are activated after 250sec as shown by the two pulses in Fig. 6 and this segment will be treated separately.

A representative signal is shown in Fig. 6, for Channel 4, which is located the 6th bay, near the tip of the boom, and measures transverse motions in the x-direction. The top plot is the measured acceleration, the bottom plot is the time varying Fast Fourier Transform (FFT), also known as the spectrogram, and is a graph of time versus frequency where the FFT amplitude is represented by the color intensity. The spectrogram is more accurate than the power spectral density (PSD) for assessing the time varying spectral content of transient disturbances.

During the night period, spikes of about 150 μg peak-to-peak occur at 15sec intervals. These spikes are correlated on the spectrogram with activity around 100 Hz, and persist throughout the whole record. This behavior could be consistent with the disturbances from the rotating tape recorder mechanisms. During this period, the background level is approximately 35μg broadband RMS, and includes the noise floor of the instrumentation which is estimated at 22μg.

During the transition time (30sec to 70sec), a snap occurs at 58 seconds into the data. This snap is characterized by a 1mg peak-to-peak impulse followed by a decayed ring down of a mode around 40 Hz. Pre-flight analysis predicted the fundamental torsional mode near that frequency. An effort in currently being undertaken to visualize the snap motions at all degrees

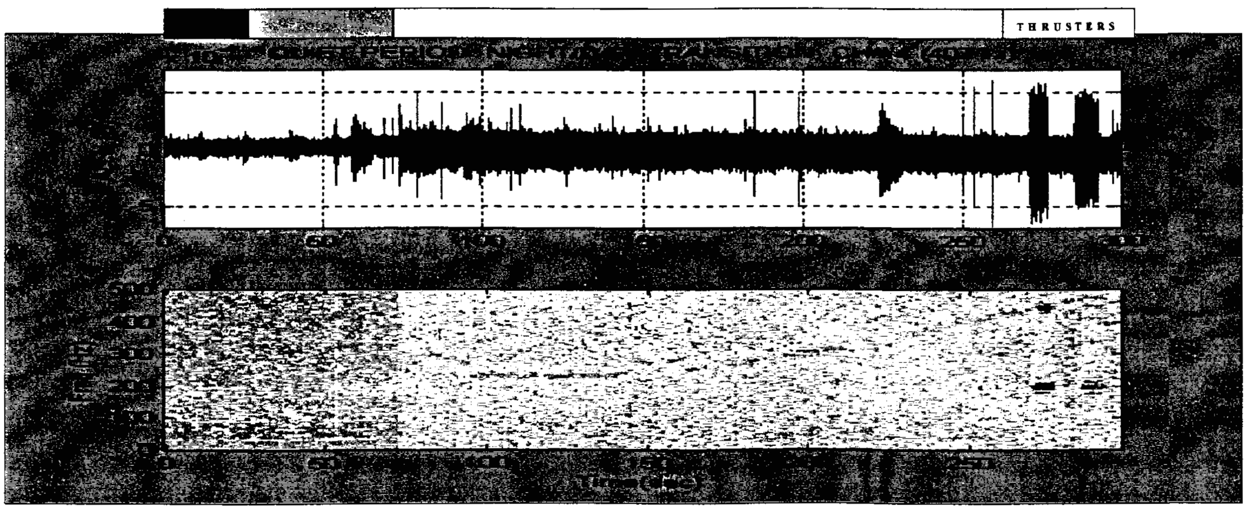

Figure 6. Acceleration Time History and Spectrogram at Ch. 4x (X-dir bending at 6th bay) during Quiet Period.

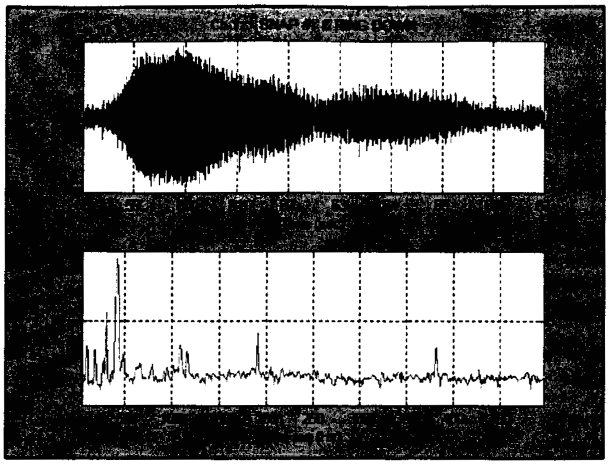

Figure 7. Impulsive boom snap at Ch. 1 (Z-dir bending at boom tip

of freedom of the boom, even those that were not measured. The motion visualization will help in interpreting the measured snap data.

The transient boom snap at 58 sec has a RMS of about 130μ. The amplitude is largest near the tip. For example is Ch.1 located at the tip of the boom, and measuring z-bending direction motions (Fig. 7), this portion of the data has a RMS of 140μg and a maximum peak-to-peak amplitude of 0.9mg. Channels away from the tip do not show an impulse at the beginning of the snap, and have responses that are lower in amplitude. The reduced amplitude away from the tip is consistent with the response of the boom in its first torsional mode. The time history data only shows a 42 Hz mode ring down without an initial impulse to excite that mode. This behavior is consistent with observed propagation attenuation effects of impulsive disturbances such as earthquakes. Based on the seismic analogy, the impulsive boom snap may have initially occurred at an unmeasured location, but has strongly excited this 42 Hz mode. Its cause has not yet been determined. A second similar event is observed at 225sec (Fig. 6).

During the transient day period (70sec to 250sec), the signal suddenly becomes very noisy and the boom seems to be in a continuous state of jitter (Fig. 6). This jitter is observed in every channel, but completely disappears in the next experiment 10 minutes later when the internal boom temperatures have stabilized. The time 74sec corresponds to the sharp rise in temperature observed in Fig. 5. The jitter has a peak-to-peak amplitude of 400μg, and an RMS of about 75μg. This persistent boom motion is characterized by a time varying frequency which increases from approximately 250Hz to 500Hz over the course of the experiment, as shown in the spectrogram in Fig. 6. Intermittent jumps in the FFT are correlated in time with other simultaneous snapping events. It is suspected that this signal is aliased through the second order anti-aliasing filter, and the signal is in fact decreasing in frequency from 750Hz down to 500Hz. This decrease in frequency could be associated with the rise in temperature during this period, which in turn changes the pre-load at the joints. A preliminary modal test performed on a single bay article uncovered a very nonlinear mode in the vicinity of 600Hz, which could be associated with the persistent boom jitter. An analysis also demonstrated that heating the truss lowers the applied pre-load because of extension of the cables.

In an effort to confirm that the jitter data was indeed mechanical, and not induced by electrical noise, a series of ground tests was performed after the boom and the electronics returned to the laboratory. The tests did not reveal any electronic anomaly, including potential grounding problems. The boom and the electronic hardware were even subjected to the same types of thermal loading profile as induced on-orbit. No snapping, be it pulse-like or persistent, was measured from the electronics or the mechanical response of the boom. Furthermore, the persistent snapping was not observed (to date) in any other portion of the flight data, although there were many other thermal transition measured. It is thus concluded that the measured data is real, that gravity impedes the boom from snapping on the ground, and that continuous background vibrations from other payloads and spacecraft mechanisms continuously exercises the joints thus relieving any locally built-up strain.

A previous interpretation of this persistent jitter proposed that the boom be in a continuous *snapping* state induced by the thermal load and redistribution of its internal strains to the minimal energy configuration. It was hypothesized that the snaps were

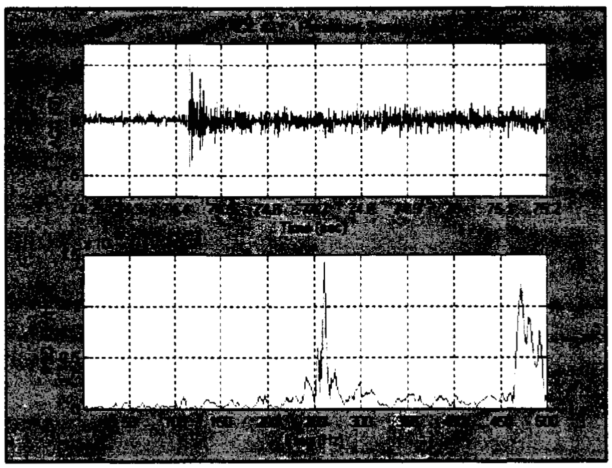

Figure 8. Beginning of Persistent Jitter at Ch. 2 (y-dir axial at boom tip).

generated when by stress relief at the joints and at all discontinuous interfaces. It should be noted that in theory any type of load could produce this effect, including mechanical load redistribution due to moving parts. A close-up of the crackling is shown in Fig. 8 for Ch. 2Y, where the event is immediately preceded by one or more large impulses at 74.5sec. In this particular channel which measures the axial motion of the boom(Ch. 2Y), the snap is characterized by a 260Hz persistent jitter frequency, and a 480Hz initial snap ring down. Other snaps with identical ring down frequencies are observed later on in the Ch.2 record. However, these snaps are not always synchronized with impulses in other channels, as they are for this particular initial pulse at 74.5sec. Most other channels for the bending motions of the boom, record a persistent jitter in the vicinity of 260Hz, but have a 190Hz initial pulse decay frequency (Ch. 4x). The different response frequencies may be an indicator of the source mechanism that triggered the event. This initial impulse is observed in some of the other channels, but not in Ch. 1 at the tip of the boom in the Z-direction. Looking at the synchronization of the pulse, it seems to have triggered in the bays near the base of the boom, but is largest at the boom to A/S interface.

A previous explanation had suggested that the initial impulse triggered an internal instability within the boom which induced continuous snapping at the joints. However, closer inspection of the persistent jitter segment reveals that the motion is not a continuous series of isolated jumps and decays, as would be expected from local snaps. In fact, after the initial impulse has subsided, the jitter is more steady state in nature, although there are intermittent large amplitude impulses (Fig 6 & 8). Hence, a more plausible explanation is that the initial snap excited the local modes of the longerons and batten struts, and that low friction and material damping allowed these modes to ring on for minutes. It is nonetheless possible that the intermittent larger snaps observed on top of the persistent jitter (Fig. 5) are continuously exciting the local strut modes until they completely dissipate by the next experiment sequence.

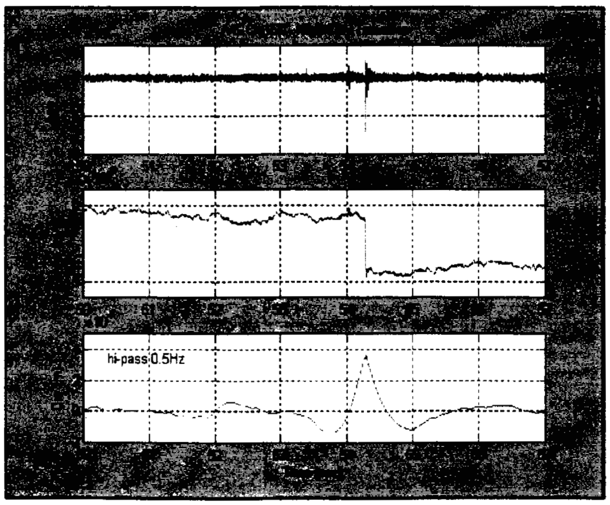

Figure 9. A/S base snap (Ch. 15).: a) acceleration (g), b, velocity (m/sec),c) displacement (m)

Another significant snap occurred at 54sec, as shown in the top trace in Fig. 9 for Ch. 15, located on the A/S node nearest to the support struts connection. Synchronization of this snap across the boom indicates that it initiated on the A/S side, with a delay of about 5millisec from the A/S (Ch.15) to the tip of the boom. The characteristic frequency of this snap is 95 Hz. The mechanism that produced this snap is unclear as each strut was tightly bolted down to the A/S with 7 bolts. The time delay is consistent with the predominant mode at the source, with frequency 95Hz (i.e., round-trip period 10.5msec), propagating over a distance of 2.5m from the base to the tip. Also the peak-to-peak acceleration is one-sided at the A/S base with amplitude 0.8mg, whereas after propagation along the boom, the pulse becomes double-sided with a peak-to-peak amplitude of 1.1mg (Fig. 6). One-sided acceleration pulses are typically associated with a jump in velocity, and a drift in the displacement. This is illustrated in the two bottom plots of Fig. 9. The velocity has a quasi-instantaneous jump of 50μm/s, and the associated displacement has a *relative* 6μm peak-to-peak motion. The displacement time history in this figure has been high-pass filtered at 0.5Hz to remove parabolic drifts due to unknown initial conditions.

The cable assemblies are also very active during the quiet period, as shown in Fig. 10. The time traces shown in this plot represent the first 3 minutes into the quiet period, and encompass the night, transition and transient day conditions. The channels shown are, a)

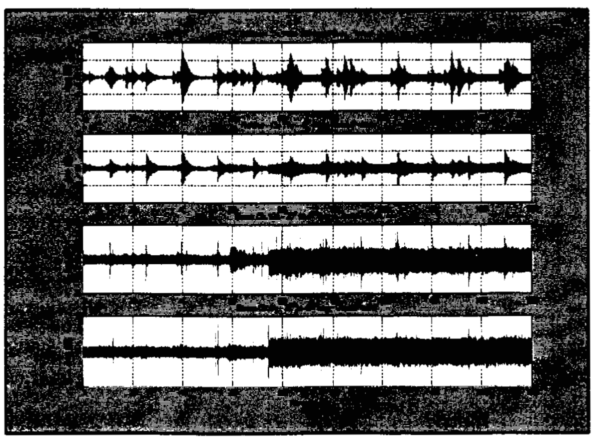

Figure 10. Cable drum modes synchronized with pulses on boom: a) Cable Ch.14x, b) Cable Ch. 11x, c) Boom Ch. 10z, d) Boom Ch. 8y.

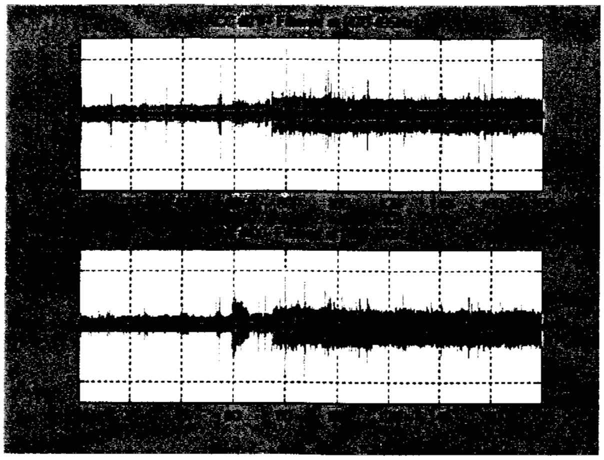

Figure 11. Narrow-Band Filters applied to flight data for characterization of transients. a) Ch. 2Y [470-495Hz]; b) Ch 4X [188-200Hz].

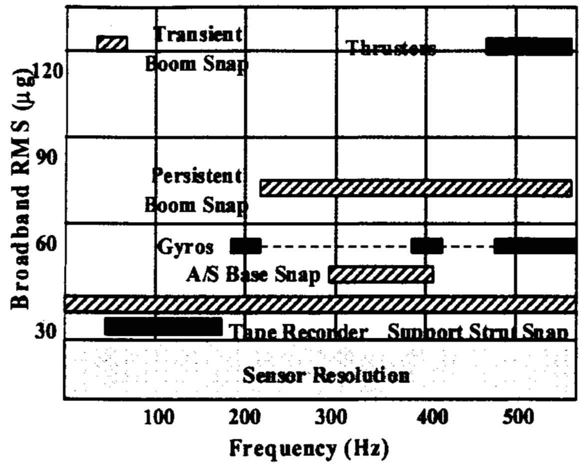

Figure 12. Characterization of boom disturbances observed during the quiet period.

Ch.14 which measures the cable drum modes in the x-dir. in the 3rd bay, b) Ch. 11 which measures the cable drum modes in the 4th bay adjacent to the previous channel, c) Ch. 10 which measures the z-bending of the boom at a node in between the 2 previous bays, and d) Ch. 8 which measures the axial y-motion of the boom in between the 2 bays. The main driver of the cable modes are the tape recorder pulses, as seen by the synchronization of the drum mode ring-downs with the regular 15-sec pulse (Fig. 10-c). Also, the response amplitudes are greater at Ch.14 (Fig. 10-a) than at Ch. 11 (Fig. 10-b) located further away from the A/S input. This is consistent with the tape recorder disturbance assumption, since disturbance attenuates over distance. Also, the cables do not respond significantly to the boom transient snap at 58sec, or the boom persistent snaps starting at 74sec. Furthermore, there are drum modes that occur in the absence of observable spikes in the boom data, such as the ring-down clusters at 110Hz and 150Hz in Ch. 14 (Fig. 10-a). This may be an indication of A/S generated disturbances that are below the noise floor of the IPEX sensors. Conversely, there are pulses measured on the boom that do not excite drum modes. One notable example is the initial pulse at the beginning of the persistent jitter period at 74sec. Hence, it might be deduced that the cables to do not respond to certain classes of structural jitter disturbances. Thus, the cable data can be used as a discriminator to detect which spikes observed in the boom response are from the tape recorders and which spikes are from structural snaps.

In an effort to categorize the snaps by their frequency content, narrow pass-band filters were applied to the time histories. Two such examples are illustrated in Fig. 11. The top shows CH. 2Y (axial motion at the tip of the boom) with a narrow band filter between [470-495] Hz. The bottom plot shows CH. 4X (bending in the 6th bay) with a narrow band filter between [188-200] Hz. In both cases, the lighter shade plot represents the unfiltered data. As can be observed, the filtered data still exhibits intermittent impulses, however some of the snaps in the unfiltered data have been removed. Hence, these narrow band filters are effective in identifying classes of impulses. Other filtering techniques, such as wavelets, will also be investigated. These might be more appropriate to characterize transient, non-harmonic, signals. A follow-on effort is also being undertaken to visualize these impulses, as to better grasp the nature and source of these disturbances.

There are still many snaps in the quiet period data that have yet to be identified. Also, the night/day transitions recorded during the A/S normal operations period need to be examined for similar snapping characteristics. These findings will be reported in the near future.

4.3. Astro-Spas Mechanical Disturbances

The latter part of the quiet period and the following next two experiments were dedicated to characterizing the Astro-Spas induced mechanical disturbances, namely, the thrusters and gyros. During the last 30 seconds of the quiet period (270-300 sec, Fig. 6), the thrusters were activated in a particular sequence with the gyros still turned off. In the following experiments, the gyros were turned back on, and there were intermittent periods when the thrusters were pulsed. During these experiments, the boom always remained in shadow, and hence, was unperturbed by thermal disturbances. Thus, it was possible to individually characterize each disturbance source. The results are

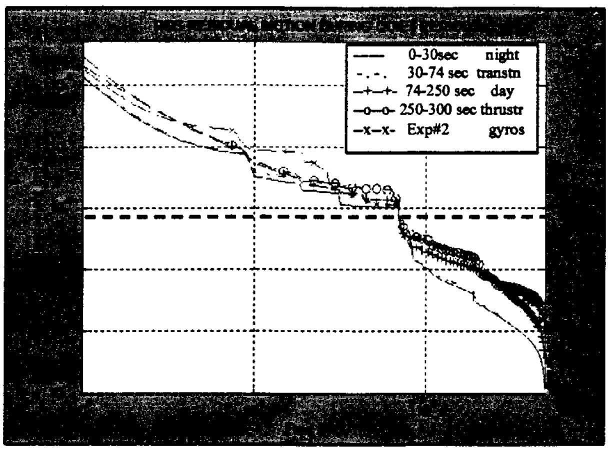

Figure 13. RMS residual motions for individual thermo-mechanical disturbance sources.

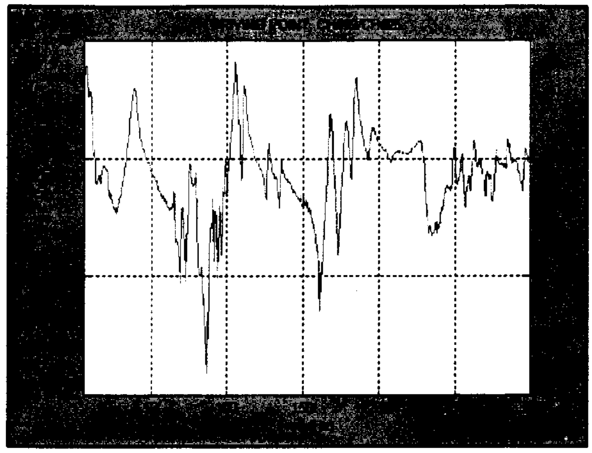

Figure 14. Driving point transfer function at shaker #1, obtained during broadband random input tests.

summarized in Fig. 12. The thrusters add about 120μg RMS broadband, to the response at the tip of the boom, with predominant contributions at 400Hz to 480Hz, which is aliased down from 520Hz – 600Hz as confirmed by the data sampled at 900Hz, and by the IPEX-I results. At the base of the boom, on the A/S, the thrusters imparted a disturbance of approximately 60μg RMS. The gyros are narrowband disturbances with components at 200 Hz, 400Hz, and 495Hz. These are aliased own from 505 Hz and 800 Hz, as confirmed by the 909Hz sampling experiments, and the pre-flight ground tests. The disturbance is largest next to the gyros at Ch. 16 with 306μg RMS, but only registered 24μg at the base of the boom inducing 50μg response at the tip. Again, propagation attenuation significantly reduced the disturbance levels of the source mechanisms. Disturbances induced by the tape recorders and the various snaps have been reported earlier, and are also summarized in Fig. 12.

Residual motions were computed for each of the thermo-mechanical disturbance sources, as shown in Fig. 13. Five different lines are drawn for the night, transition, and transient day thermal conditions, as well as for the thrusters and the gyro mechanical disturbances. The data for each line represents the RSS value of the reverse cumulative PSDs over all acceleration channels, divided by ω^4 to integrate into displacements. As expected, the night period is the quietest by a factor of 5 in certain regions. Overall, the boom is relativity quiet in a RMS sense, since above 100Hz the residual motions are less than 10 nm, and thus fit within the current SIM stability requirements. HOWEVER, it should be remembered that RMS metrics are not appropriate for transient disturbances, since they smear out any large spikes. Such low numbers do not preclude milli-g acceleration pulses, 50 μm/s velocity jumps and μm level instantaneous motions (Fig.9). When designing precision structures, it is strongly advised to include requirements that also specify peak allowable motions.

4.4. Structural Dynamic Characterization

The 2 mechanical shakers located at the tip of the boom were used to perform modal tests for on-orbit characterization of the boom dynamics. Fourteen 5-minute tests were performed, including five broadband random input tests between 9Hz and 303Hz, at two input levels of 0.101lbf and 0.0126lbf. Narrowband step-sine tests were also performed in bands of 12 Hz to 35.7Hz, 34.5Hz to 56 Hz, and 54.8Hz to 90.6Hz.

Dynamic properties of the boom have yet to be extracted from the flight tests. However, the data was verified, and a sample acceleration transfer function is shown in Fig. 14 for the driving point at shaker #1. The experiment was a broadband burst random test between 9.5Hz and 303Hz, performed at the high force level of 0.1lb. The experiment was a total of 17 cycles over 5minutes, with 10 seconds of random shaking followed by 8 seconds off. According to pre-flight analytical predictions the large peak at 38.5Hz is close to the first torsional mode. The damping assessed by the half-power bandwidth method is approximately 4%. Post-flight testing of the boom is currently being performed with the same cabling configuration as on orbit. The ground tests only show damping of 1%, thus eliminating the hypothesis that cables alone are responsible for the increased damping. Another potential cause for the increase of on-orbit damping is the friction mechanism of joints and cable ties in zero-g. Assessing what causes the increased damping on-orbit will be important for the accurate response prediction to on-board disturbances.

5. CONCLUSION

The IPEX experiments demonstrated the high-frequency nanometer thermo mechanical stability of the ASTRO-SPAS platform and a representative boom on-orbit. Preliminary data indicates that all the instrumentation functioned as planned during the flight, and that the IPEX experiments were successful. The broadband acceleration RMS levels both on the ASTRO-SPAS and the boom were in the hundreds of micro-G's, thus confirming their suitability for Origins-class payloads. Analyses have been performed that assess the disturbance contributions for spacecraft mechanisms such as gyros and thrusters, as well as thermal disturbances.

Propagation attenuation of ***transient*** disturbances was shown to significantly decrease in amplitude and change in aspect away from the source. This may be a direct result of wave dispersion effects, as well as the higher damping observed on-orbit. Thus implying that transient disturbances would mostly impact mechanical and optical components located in the vicinity of the disturbance source. Furthermore, it has been shown that traditional spectral methods are not appropriate to gauge the intensity of the transient disturbances. Some snaps have been shown to have large instantaneous velocities and micron displacements, while not significantly perturbing the μg RMS levels. All these issues are important when designing vibration attenuation strategies and predicting performances of sensitive opto-mechanical elements.

Foremost, IPEX demonstrated the existence of internal snaps in a pre-loaded joint-dominated structure, thus invalidating conventional wisdom which dictated that preload prevents all motion and stabilizes the microdynamics. It was noted that temperature variation is only one of the ways load is internally imparted to a structure. In theory, internal mass and inertia redistribution due to moving elements could trigger the same microdynamic snap mechanisms. It was also shown that internal snaps are not all lurch-like events with single-mode ring down. Some microdynamic events are persistent, others occur prior to the abrupt thermal load variation, and others initiate away from the boom near the bolted interface connections. These observations are not unlike the phenomena observed after earthquakes, with aftershocks occurring years later on unconnected faults. Although the source of these specific snaps has yet to be identified and modeled, it is suspected that they occur along discontinuous contacting surfaces [6]. This is not restricted to the joint-dominated truss architecture of the IPEX boom. Discontinuous surfaces are also prevalent in composite structures, which are known to snap under thermal cycling.

Nevertheless, the IPEX data demonstrated that even in the presence of microdynamic events, the ASTRO-SPAS spacecraft and the AEC-ABLE ADAM mast boom provide the level of stability required for future Origins mission, and as such, establish a cornerstone for all future precision optical space system designs.

6. ACKNOWLEDGEMENTS

This work was performed at the Jet Propulsion Laboratory, California Institute of Technology, under contract with the National Aeronautics and Space Administration. The author would like to thank R. A. Laskin, Interferometry Technology Program, and the IPEX team of JPL, as well as the DASA ASTRO-SPAS team at KSC for their guidance and commitment of resources that made this work possible.

7. REFERENCES

1. Naderi, F., "NASA's ORIGINS Program", *Proc. SPIE Astronomical Telescopes and Instrumentation Conference*, Kona Hawaii, March 1998, N0. 3350-125 (to be published).

2. Blair, M., and J. Sills, "Hubble Space Telescope On-Orbit System Identification", *Proc. 12th International Modal Analysis Conf.,* Honolulu, Ha, Feb 1994, p. 663-669.

3. Eilers, D., U. Lubbers, and F. De Rose, "EURECA-MMS Microgravity Measurement Subsystem Post-Flight Evaluation, Final Report", ESA/ESTEC Contract report N0. 10016, Bremen Germany, Dec. 1994.

4. Umland, J. and M.Levine, "Interferometry Program Experiment #1: Flight Data Analysis", European Conference on Spacecraft Structures and Materials and Mechanical Testing, Nov. 1998, Braunschweig, Germany.

5. H. Gutierrez and M. Levine, "Analysis of IPEX-2 Pre-Flight Ground Integration Test Data", ", NASA Jet Propulsion Laboratory Internal Document **JPL D-14905**, Oct. 1997, Pasadena CA.

6. Peterson, L.D. "Submicron Precision Deployable Spacecraft Structures: Final Report" University of Colorado, Boulder. Report no. CU-CAS-97-24, December 1997.